# Electronic structure and magnetic anisotropies in orthorhombic multiferroic $YMnO_3$ thin films



2009 J. Phys.: Conf. Ser. 150 042062

(http://iopscience.iop.org/1742-6596/150/4/042062)

Journal of Physics: Conference Series **150** (2009) 042062 doi:10.1088/1742-6596/150/4/042062

# Electronic Structure and Magnetic Anisotropies in Orthorhombic Multiferroic $YMnO_3$ Thin Films

**C C Hsieh[1,*], T H Lin[1], H C Shih[1], J -Y Lin[2], C –H Hsu[3], C W Luo[1], K H Wu[1], T M Uen[1], and J Y Juang[1]**

[1] Department of Electrophysics, National Chiao Tung University, Hsinchu, Taiwan

[2] Institute of Physics, National Chiao Tung University, Hsinchu, Taiwan

[3] National Synchrotron Radiation Research Center (NSRRC), Hsinchu 30076, Taiwan

E-mail: cchsieh.ep90g@nctu.edu.tw

**Abstract**. Thermodynamically $YMnO_3$ (YMO) can only exist with hexagonal structure at ambient conditions. In this study, we demonstrate that the stain between film and substrate can play an important role in forming orthorhombic YMO (o-YMO). o-YMO films with nearly perfect crystallographic orientation alignment were obtained on $LaAlO_3$(*110*) substrates. These films allow us to unambiguously disclose the intrinsic magnetic property and electronic structure anisotropies along different crystallographic orientations. The antiferromagnetic (AFM) phase transition was around 42 K. Moreover, we observed a signature of spin reordering at lower temperatures when the applied field was parallel to the a- or c-axis. On the other hand, only the AFM transition was observed when the field is parallel to the b-axis. By comparing the X-ray absorption spectroscopy (XAS) results to standard manganese oxides, $YMnO_3$ exhibits the dominant $Mn^{+3}$ characteristics as that obtained from the standard $Mn_2O_3$ powder. The polarization dependent XAS also revealed anisotropic bonding behavior along each crystalline axis.

## 1. Introduction

In recent years, perovskite manganites $RMnO_3$ (R = rare earth and Y) had been widely investigated owing to the rich and interesting physical properties involved in these materials [1-5]. Extensive researches have already indicated the intimating interplays involving spin, orbital and charge orderings in the hole-doped $LaMnO_3$ manganites in giving rise to the colossal magnetoresistance (CMR) [6-11]. With further reduced rare-earth ionic size, the $RMnO_3$ compounds have revealed even richer and interesting physical behaviors. For instance, with the ionic size reducing form 1.22Å (R = La) to 0.94Å (R = Lu) the magnetic phase diagram has implicated complicate competitions involving the Jahn-Teller distortion, ferromagnetic and antiferromagnetic interactions.

However, understanding the correlations between the electronic structure and the Jahn-Teller distortion is still an important topic. The Jahn-Teller distortion plays an important role in variation of Mn-O-Mn bond angle and Mn-O bond length in the $MnO_6$ perovskite structure. According to Tachibana et al., the variation of lattice constant and bond length by Jahn-Teller distortion can also be anisotropic along different crystalline axes of orthorhombic $RMnO_3$ [5]. This may also infer the anisotropic bonding behavior with small ionic size of rare earth in $RMnO_3$. Unfortunately the single crystal $RMnO_3$ (for R = Y and smaller rare earth Ho to Lu) with orthorhombic structure are not

 

available at present and current results concerning the electronic structures of the orthorhombic $RMnO_3$ (with R = Y to Lu) are all obtained from samples fabricated via high temperature, high pressure synthesis [3; 12-15], thus there are still some outstanding issues remaining to be clarified. In this chapter, we use thin films with orthorhombic structure grown on LAO(110) substrates to probe the anisotropic bonding behavior along each crystalline axis.

## 2. Experiment

The thin film was prepared by pulsed laser deposition process. [16] In order to tune the optimum conditions, the KrF excimer laser was operated at a repetition rate of 1~10 Hz with an energy density of 2-5 J/cm$^2$ and the substrate temperature ($T_s$) was varied between 700 °C up to 880 °C with the oxygen partial pressure being controlled between background pressure ($10^{-6}$ torr) to 0.3 torr during deposition. The structural characteristics of the films were measured by x-ray diffraction (XRD) θ-2θ and Φ scans. The X-ray absorption near edge spectroscopy (XANES) were collected by the fluorescence electron yield (FY) mode with resolution 0.15 eV

## 3. Results and discussions

Figure 1 showed the XRD θ-2θ patterns of the YMO films deposited at different substrate temperature ($T_s$) on single crystalline (LAO(110)) substrates. In the figures, the data clearly reveal that all the films are orthorhombic phase of YMO. We could clear found the thin films reveal b-axis oriented with orthorhombic structure normal to the substrates. The orthorhombic-YMO(020) (o-YMO(020)) were obtained over the whole $T_s$ range (700-880 °C) practiced. It is also evident that the crystalline quality is progressively improved with increasing $T_s$. Thin film sample of the highest deposition temperature which had best crystalline quality was choosen to characterized the later behavior.

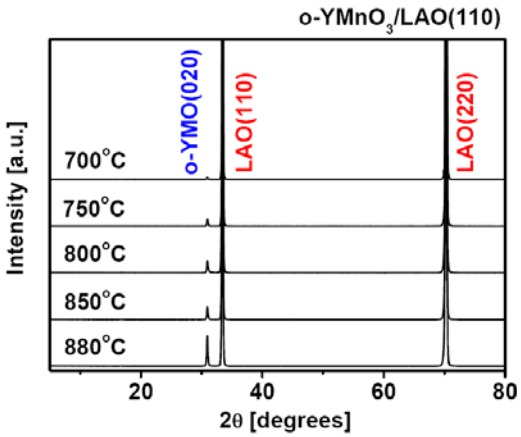


**Figure 1.** The XRD θ-2θ patterns of o-YMO thin films grown on LAO(110) substrates as s function of the deposition temperature. All films were controlled to have the same thickness (180 nm) and an optimum oxygen partial pressure of 0.1 torr to delineate the relation between temperature and the degree of crystallization in the deposition process.

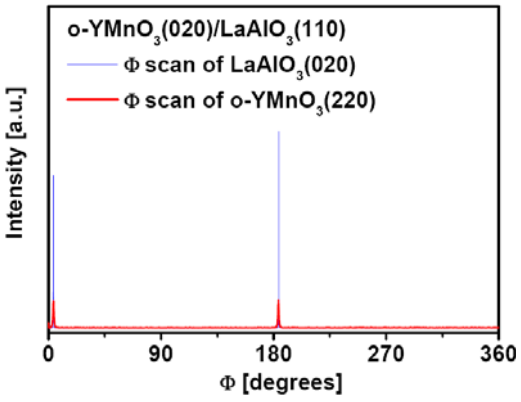


**Figure 2.** The XRD Φ-scan patterns of *o*-YMO thin films deposited at 880 °C on LAO(110) substrates. The results clearly display the intimate epitaxial relationship between film and substrate, as well as the distinct film orientation characteristics.

In Figure 2, the sample o-YMO(020)/LAO(110) examined the in-plane alignments between thin film and substrates with XRD Φ-scan data. The off-normal brag's peaks of thin film's o-YMO(220) and LAO substrate's LAO(020) emerged at the same Φ degrees. By considering the mismatch and Φ-

scan data, we could find that a-axis of o-YMO aligned with the $[1\bar{1}0]$ direction of LAO(110) substrates and the c-axis of o-YMO aligned with the $[001]$ direction of LAO(110) substrates. Detailed discussions had been reported in the further experiments. The Φ-scans on the *o*-YMO(220) diffraction peak and the LAO(020) peak indeed clearly indicate the two-fold symmetry for pure orthorhombic structure and the excellent epitaxial relations between film and substrates.

The Mn L edge XANES spectra of standard powders MnO, $Mn_2O_3$, and $MnO_2$ standard was showed in Figure 3(a) and the data were showed with TEY mode. All of these standard powders showed two broad multiplet $L_2$ and $L_3$ peak for the main behaviors, and the Mn-$L_3$ and Mn-$L_2$ located in the range of 640~650eV and 650~660eV which was separated by spin-orbital interaction respectively. There was a little difference in the Mn-$L_3$ peak between theses powders. By comparing with trivalent manganese, the main peak shift to lower energy and thicker with the divalent manganese, it shift to higher energy with the quadrivalent manganese. Owing to this scenario, we could easily clarify the valence in the $RMnO_3$ compounds. Figure 3(b) showed Mn L edge XANES spectra for and thin film sample $LaMnO_3$(001)/$SrTiO_3$(001) and *o*-YMO(020)/LAO(110) and it was probed with linear polarized x-ray. The electric field was set parallel to *a*-*b* plane in $LaMnO_3$ and E//a-axis, E//b-axis, and E//c-axis in o-YMO thin films. By comparison with the a-b plane in $LaMnO_3$ and similar partial weight (E//a and E//b) in o-YMO, we could find the Mn-$L_3$ peak shift to left about 0.3 eV and revealed sharper. When the electric field parallel to c-axis, there were two peaks at the top of Mn-$L_3$ and separated about 0.5 eV. Sometimes, $LaMnO_3$ thin film on $SrTiO_3$(001) showed like behaviors for its light distorted $GdFeO_3$ type and it would reveal nearly bonding isotropy. The spectra of o-YMO showed the anisotropic electronic structure which was different to the $LaMnO_3$ thin films.

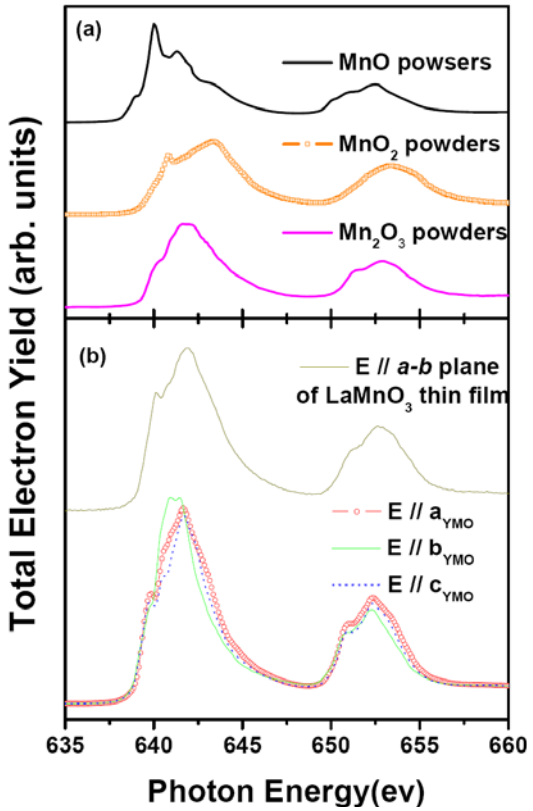


**Figure 3.** The XRD θ-2θ patterns of o-YMO thin films grown on LAO(110) substrates as s function of the deposition temperature. All films were controlled to have the same thickness (180 nm) and an optimum oxygen partial pressure of 0.1 torr to delineate the relation between temperature and the degree of crystallization in the deposition process.

## 4. Summary

We have prepared o-YMO highly b-axis normal originated thin films on LAO(110) substrates and the thin films revealed two-fold symmetry as an orthorhombic structure. The thin film allows us to

unambiguously disclose the intrinsic XANES spectra along different crystallographic orientations and the data show the bonding anisotropy behaviors.

**Acknowledgement**

This work was supported by the National Science Council of Taiwan, ROC under Grants: NSC 95-2112-M-009 -035 -MY3, NSC 95-2112-M-009 -038 -MY3, NSC95-2112-M-213-005, and 96W801. And we thanks for the XRD Φ-scan experiments support by BL13A beam line in National Synchrotron Radiation Research Center in Taiwan.

## References

1. Kimura T, Ishihara S, Shintani H, Arima T, Takahashi KT, Ishizaka K, Tokura Y (2003) Physical Review B 68:060403
2. Goto T, Kimura T, Lawes G, Ramirez AP, Tokura Y (2004) Physical Review Letters 92:257201
3. Prellier W, Singh MP, Murugavel P (2005) Journal of Physics-Condensed Matter 17:R803
4. Zhou JS, Goodenough JB (2006) Physical Review Letters 96:247202
5. Tachibana M, Shimoyama T, Kawaji H, Atake T, Takayama-Muromachi E (2007) Physical Review B 75:144425
6. Mizokawa T, Fujimori A (1995) Physical Review B 51:12880
7. Ishihara S, Inoue J, Maekawa S (1997) Physical Review B 55:8280
8. Murakami Y, Hill JP, Gibbs D, Blume M, Koyama I, Tanaka M, Kawata H, Arima T, Tokura Y, Hirota K, Endoh Y (1998) Physical Review Letters 81:582
9. Sánchez MC, Subías G, García J, Blasco J (2003) Physical Review Letters 90:045503
10. Chen SF, Chang WJ, Hsieh CC, Liu SJ, Juang JY, Wu KH, Uen TM, Lin JY, Gou YS (2006) Journal of Applied Physics 100:113906
11. Chang WJ, Hsieh CC, Juang JY, Wu KH, Uen TM, Gou YS, Hsu CH, Lin JY (2004) Journal of Applied Physics 96:4357-4361
12. Iliev MN, Abrashev MV, Lee HG, Popov VN, Sun YY, Thomsen C, Meng RL, Chu CW (1998) Physical Review B 57:2872
13. Lorenz B, Wang YQ, Sun YY, Chu CW (2004) Physical Review B 70:212412
14. Kim J, Jung S, Park MS, Lee SI, Drew HD, Cheong H, Kim KH, Choi EJ (2006) Physical Review B 74:052406
15. Lorenz B, Wang YQ, Chu CW (2007) Physical Review B 76:104405
16. Hsieh CC, Lin TH ,Shih HC , Hsu C-H, Luo CW, Lin J-Y, Wu KH, Uen TM, Juang JY (2008) revised with Journal of Applied Physics